

Retraction

Retracted: Digital Image Automatic Recognition and Tracking Based on Electronic Derotation Algorithm

Advances in Multimedia

Received 15 August 2023; Accepted 15 August 2023; Published 16 August 2023

Copyright © 2023 Advances in Multimedia. This is an open access article distributed under the Creative Commons Attribution License, which permits unrestricted use, distribution, and reproduction in any medium, provided the original work is properly cited.

This article has been retracted by Hindawi following an investigation undertaken by the publisher [1]. This investigation has uncovered evidence of one or more of the following indicators of systematic manipulation of the publication process:

- (1) Discrepancies in scope
- (2) Discrepancies in the description of the research reported
- (3) Discrepancies between the availability of data and the research described
- (4) Inappropriate citations
- (5) Incoherent, meaningless and/or irrelevant content included in the article
- (6) Peer-review manipulation

The presence of these indicators undermines our confidence in the integrity of the article's content and we cannot, therefore, vouch for its reliability. Please note that this notice is intended solely to alert readers that the content of this article is unreliable. We have not investigated whether authors were aware of or involved in the systematic manipulation of the publication process.

Wiley and Hindawi regrets that the usual quality checks did not identify these issues before publication and have since put additional measures in place to safeguard research integrity.

We wish to credit our own Research Integrity and Research Publishing teams and anonymous and named external researchers and research integrity experts for contributing to this investigation.

The corresponding author, as the representative of all authors, has been given the opportunity to register their agreement or disagreement to this retraction. We have kept a record of any response received.

References

- [1] M. Gao, "Digital Image Automatic Recognition and Tracking Based on Electronic Derotation Algorithm," *Advances in Multimedia*, vol. 2021, Article ID 6111812, 7 pages, 2021.

Research Article

Digital Image Automatic Recognition and Tracking Based on Electronic Derotation Algorithm

Meirong Gao 

College of Physics and Optoelectronic Technology, Baoji University of Science and Arts, Baoji, Shaanxi 721016, China

Correspondence should be addressed to Meirong Gao; yanglei@bjwxy.edu.cn

Received 24 August 2021; Accepted 29 October 2021; Published 8 December 2021

Academic Editor: Michel Kadoch

Copyright © 2021 Meirong Gao. This is an open access article distributed under the Creative Commons Attribution License, which permits unrestricted use, distribution, and reproduction in any medium, provided the original work is properly cited.

With the continuous development of my country's social economy, the ways to acquire images have become more and more abundant. How to effectively process, manage, and mine images has become a major and difficult problem in research. In view of the difficult problem of image recognition, the electronic derotation algorithm is introduced in this study, by combing and monitoring the edge features, establishing a corresponding sample database, analyzing the edge features of the image, and performing effective and stable tracking, so as to realize the automatic recognition and tracking of the digital image. The simulation experiment results show that the electronic derotation algorithm is effective and can support the automatic recognition and tracking of digital images.

1. Introduction

With the continuous development of my country's society and economy, the methods for acquiring digital images have been greatly improved, such as traditional photography, modern remote sensing photography, and other technologies, but how to process the acquired images and information mining have become important research hotspots and difficulties [1–5]. Image recognition and mining are widely used, such as judging the growth cycle and growth situation of crops from the acquired images, judging the scale and development direction of urban construction from the acquired images. There have been certain applications and research in various aspects in image-based recognition, tracking, and mining [6–8]. In terms of mechanical operation, image recognition can be used to track mechanical operations, ensure the safety of mechanical production, improve the corresponding mechanical production efficiency, realize the automation of mechanical processing, and improve the level of mechanical manufacturing in the manufacturing industry [5, 9, 10].

It should be noted that when acquiring images, due to the difference in the specific location of the image acquisition and the state of the equipment, a certain amount of shaking or

rotation is prone to occur, which will affect the quality of the image, therefore causing the user to misjudge and miss the corresponding key information. For the automatic tracking part of the image, the stability and accuracy of the image tracking will occur due to the unstable image, resulting in a large error in the final result. Therefore, in the image processing, the derotation is extremely important [11, 12]. The so-called derotation can be divided into three methods: optical, electronic, and physical derotation according to the way of image acquisition. For optical derotation, optical equipment is used to eliminate lens; there are several characteristics of using electronic derotation. The derotation image transformation and the original image coordinate transformation are accurately analyzed, and it has the advantages of lower cost, strong reliability, and high efficiency.

Therefore, in view of the current automatic recognition and tracking of digital images, the electronic derotation algorithm is introduced in an attempt to sort out the flow of edge features and sort out the monitoring process, establish a corresponding sample database, analyze the edge features of the image, and perform effective and stable tracking, so as to achieve the automatic recognition and tracking of images, aiming to explore the effectiveness of automatic image recognition.

2. Principle of Image Derotation

The essence of the derotation of the acquired image is to perform the rotation transformation according to the corresponding angle transformation, and the original image is rotated according to the angle. Therefore, in general, the feature of the image electronic derotation algorithm is based on the rotation transformation of the image. The final target image is obtained by transforming the original image into another angle. But for electronic derotation, the angle of the rotation operation of the transformation is less than 1, but because the coordinates need to be round, the image problem after the rotation is prone to occur.

In order to perform image rotation, the method of reverse rotation is usually used to calculate the pixel coordinates (x' , y') of the specific image after rotation, the corresponding pixel coordinates (x , y) of the original image, and the specific transformation formula is

$$\begin{cases} x_0 = x + (y' - y_0)\sin\theta - (x' - x_0)\cos\theta \\ y_0 = y - (y' - y_0)\cos\theta - (x' - x_0)\sin\theta \end{cases} \quad (1)$$

In the formula, for the pixel coordinate value of each image after rotation, it is changed according to formula (1) to find the pixel coordinate value of the corresponding image.

According to formula (1), the cos function and sin function only need to be calculated once, and the corresponding constants can be saved accordingly, so that they can be reused and save the amount of calculation. This part needs to be improved, and the floating point multiplication and floating point addition need to be improved, thereby increasing the processing speed.

After rotating the image, it should be noted that the complete structure of the image does not change, that is, the specific direction and specific relative distance between pixels cannot be changed. Therefore, the corresponding formula can be used to calculate the pixel coordinates.

Assuming that the image is rotated in a clockwise direction, the offset of the horizontal axis X axis direction, relative to the horizontal direction, and the vertical axis can be calculated using the cos and sin functions, respectively; the pixels in the vertical axis direction are calculated quantitatively with sin and cos functions, respectively, relative to the horizontal axis and vertical axis offsets of the original point [13, 14].

Therefore, whether it is a forward or reverse rotation, all the pixel values of the image can be calculated by reasoning using the above process, so as to determine the position of the pixel, but it should be noted that except for the initial pixel needing floating point multiplication, the rest of the subsequent calculations are completed by floating point addition, which saves calculation time and improves calculation efficiency.

However, in the actual electronic derotation process, due to floating point calculations, there will be decimal points in adjacent calculated pixels, which makes it impossible to obtain accurate gray values. Therefore, the industry has gradually introduced interpolation methods to solve the problem of decimal floating point. The most common ones

are the nearest neighbor interpolation method, bilinear interpolation method, and cubic convolution interpolation method [15, 16].

2.1. The Nearest Neighbor Interpolation Method. This method essentially samples the gray value according to the sampled points. The algorithm is less complex, and the operation efficiency is faster, but meanwhile, this brings a poor interpolation effect, limited image quality, and prone to blur. Some experts have pointed out that the maximum error may exceed 50% of the error.

2.2. Bilinear Interpolation Method. The characteristic of this method is to perform interpolation in two different directions according to the 4 points around the sample. Its advantage is that the accuracy of interpolation is high, and the complexity of the algorithm is relatively low. Therefore, it is relatively easy to be accepted.

2.3. Cubic Convolution Interpolation Method. This method essentially uses the cubic sampling function $S(\omega)$ for interpolation approximation and uses 16 points around the sample for sampling interpolation. The cubic function is used for approximation, which brings high complexity calculations, the long calculation time, which is not suitable for real-time processing of the image.

Each of these three methods has its own advantages and disadvantages. The specific method of image electronic derotation needs to be selected according to actual needs, while considering the comprehensive hardware conditions.

3. Automatic Recognition and Tracking of Image

3.1. Feature Extraction for Image Recognition. For the feature extraction of automatic image recognition, the specific process is given as follows, taking a mechanical drill bit as an example:

First, perform threshold segmentation on the drill bit image and extract the moving image target of the drill bit, and on this basis, perform wavelet transform processing on the input drill bit moving image target and use the following formula to calculate:

$$F_{(i,j)}(k,l) = \left\| I(i,j) \cdot G_{(i,j)}(k,l) \right\|, \quad (2)$$

$$\eta_{pq} = \frac{\mu_{pq}}{\mu_{00}}, \gamma = \frac{p+q}{2} + 1, p+q = 2, 3, \dots$$

For the definition of the central order of the moving image, the specific formula is

$$G_x = V_{11} \times V_{T1} + V_{12} \times V_{T2} + V_{13} \times V_{T3} + V_{14} \times V_{T4} + V_{15} \times V_{T5} \\ + V_{16} \times V_{T6} + V_{17} \times V_{T7} + V_{18} \times V_{T8} + V_{19} \times V_{T9}. \quad (3)$$

Among them, the coordinates of the moving image of the drill bit are represented by (\bar{x}, \bar{y}) .

Define the following four moments that are invariant to translation, rotation, and scale transformation:

$$\begin{aligned}\phi &= \eta_{20} + \eta_{02}, \\ \phi &= (\eta_{20} - \eta_{02})^2 + 4\eta_{11}^4, \\ \phi &= (\eta_{30} - \eta_{12})^2 + (3\eta_{21} - \eta_{03})^2, \\ \phi &= (\eta_{30} + \eta_{12})^2 + (\eta_{21} + \eta_{03})^2.\end{aligned}\quad (4)$$

The pixel probability model of any pixel of the moving image at a certain moment can be specifically calculated by the following formula:

$$p(X_{ij}^t) = \sum_{s=B,F} p_s(X_{ij}^t | \theta_{ij,s}^t). \quad (5)$$

The background mixing model of moving image pixels in formula can be calculated by the following formula:

$$p_b(X_{ij}^t) = \sum_k w_{ij,b,k}^t \times \eta(X_{ij}^t, \mu_{ij,b,k}^t, \Sigma_{ij,b,k}^t). \quad (6)$$

From the background mixing model of the drill bit motion image, the submodel with the maximum fitness value can be found as the current frame background distribution model of the drill bit motion image, and equation (7) is used to calculate; the pixel (i, j) of the bit motion image at time (t) can be obtained, which belongs to conditional probability of the background:

$$\eta(X, \mu, \Sigma) = \frac{1}{(2\pi)^{(n/2)} |\Sigma|^{(1/2)}} \exp\left(-\frac{1}{2}(X - \mu)^T \Sigma^{-1} (X - \mu)\right), \quad (7)$$

where X represents the feature vector of the pixel of the drill bit moving image, n represents the dimension of the feature vector, and μ and S represent the mean value and covariance matrix of the conditional probability, respectively.

Based on the pixel prior probability of the acquired motion image of the drill bit, the pixel is judged as shown in the following formula:

$$\begin{aligned}p(C_B) &= \frac{n_B}{8}, \\ p(C_F) &= 1 - p(C_B),\end{aligned}\quad (8)$$

where $p(C_B)$ represents the prior distribution density function of pixels $p(C_B)$ in the motion image of the drill bit, and $p(C_F)$ represents the prior distribution density function of pixels $p(C_B)$ in the motion image of the drill bit. If $p(C_B) \geq p(C_F)$, the pixel is classified as background; otherwise, it is foreground.

After the moving image background is obtained, the current frame of the drill moving image is subtracted from the drill moving image background to obtain the candidate drill moving image target, which can be expressed as

$$p_u(y) = C_h \sum_{i=1}^n k\left(\left\|\frac{y - x_i}{h}\right\|^2\right) \delta[b(x_i) - u]. \quad (9)$$

3.2. Moving Image Target Detection. The gray value of each image of the moving image frame obeys the distribution of mean μ and variance σ , and the Gaussian distribution of the pixels of each drill moving image is a single variable [17–19]. The probability model of each pixel of the drill bit image frame to form a normally distributed target and background can be specifically calculated by the following formula:

$$p(x|\omega_i) = \frac{1}{\sqrt{2\pi}\sigma} \exp\left\{-\frac{1}{2}\left(\frac{x - \mu}{\sigma}\right)^2\right\}, \quad (10)$$

where ω_i represents the gray information feature value of the moving image of the drill bit.

In the $K=2, 3, \dots, L$ frame, the update formula of the mean value and variance in the drill bit moving image target (background) model is as follows.

$$\begin{aligned}\text{Mean: } \mu'_{K+1} &= (K-1/K)\mu'_{K+1} + (1/K)\mu_K. \\ \text{Variance: } \sigma_{K+1}^2 &= (K-1/K)\sigma_K^2 + (1/K)\sigma_K^2.\end{aligned}$$

In the $K=L+1$ frame, the parameter update formula in the moving image target (background) model of the drill is as follows:

$$\text{Mean: } \mu'_{K+1} = (1-\rho)\mu'_K + \rho\mu_K,$$

Variance: $\sigma_{K+1}^2 = (1-\rho)\sigma_K^2 + \rho\sigma_K^2$, where $\mu_K = (1/N_K) \sum_{j=1}^{N_K} I_j$ and $\sigma_K^2 = (1/N_K) \sum_{j=1}^{N_K} (I_j - \mu_K)^2$, respectively, represent the statistical mean and variance of the target (background) points in the drill moving image of the K^{th} frame, μ'_K and σ_K^2 represent the mean and variance of the Gaussian model used to determine the target (background) sample points in the K^{th} frame of the drill moving image, N_K represent the number of sample points of the bit moving image target (background), I_j represents the gray value of each sample point of the bit image, and ρ represents the update rate.

The Kalman filter is used to predict the target position of the drill bit moving image, and the motion covariance can be expressed as shown in the following formula:

$$\hat{X}_{K+1} = AX_K. \quad (11)$$

The target position of the drill bit moving image is predicted through combining formula (11) to obtain the true center position Z_{K+1} , and the filter equation for tracking the drill bit moving image target is shown in the following formula:

$$X_{K+1} = \hat{X}_{K+1} + G_{K+1}(Z_{K+1} - \hat{Z}_{K+1}). \quad (12)$$

3.3. Automatic Tracking of Drill Bits Based on Image Recognition. To classify the multitargets of the drill bit moving image, the Bayesian formula is used to calculate, and the posterior conditional probability of the drill bit moving image is obtained, which can be expressed as

$$\frac{P(\omega_i|x) = P(x|\omega_i)P(\omega_i)}{\sum_{i=1}^2 P(x|\omega_i)P(\omega_i)}, \quad (13)$$

where $i=1, 2$, $P(\omega_1|x)$ represents the target model of the moving image of the drill bit, and $P(\omega_2|x)$ represents the background model of the moving image of the drill bit. On

this basis, formula (8) is transformed combining formula (11), the initial position of the drill bit moving image target is given, and the target model is established using the gray information, and the posterior conditional probability judgment is performed for each sample point $I'(i, j)$ of the drill bit moving image of the K^{th} frame, the confidence map L_K of the drill movement can be obtained as shown in the following formula:

$$L_K(i, j) = \frac{P(\omega_1|x)}{P(\omega_2|x)}. \quad (14)$$

Combining the mean shift theory, the peak point of the confidence map of the drill motion is found, and the calculation result can be expressed as

$$\begin{aligned} \bar{I}^{t+1} &= \frac{\sum_{(i,j) \in N_C} \bar{I}^t L_K(i, j)}{\sum_{(i,j) \in N_C} \bar{I}^t L_K(i, j)}, \\ \bar{J}^{t+1} &= \frac{\sum_{(i,j) \in N_C} \bar{J}^t L_K(i, j)}{\sum_{(i,j) \in N_C} \bar{J}^t L_K(i, j)}, \end{aligned} \quad (15)$$

where N_C represents the neighborhood centered on the peak point (\bar{I}^t, \bar{J}^t) of the drill motion confidence map, the initial value (\bar{I}^0, \bar{J}^0) represents the predicted value obtained by Kalman filter filtering, and (i, j) , respectively, represent the coordinates of each point in the drill motion confidence map L_K .

After the peak value of the drill bit motion confidence map is obtained by the mean shift algorithm, the drill bit motion image window size of the previous frame is the initial value, and the optimum point of the motion image target is framed. The specific calculation is carried out using the following formula:

$$F = e_i \sum_{i=1}^N p_u(y) L_K(\bar{I}^{t+1}, \bar{J}^{t+1}), \quad (16)$$

where e_i represents the size of the drill moving image window of the previous frame, and the automatic tracking of the drill moving image is completed according to the window size of the previous frame.

4. The Overall Structure of the System

The system is mainly composed of four modules: image information acquisition module, image target information recognition and tracking module, image storage module, and image recognition and tracking result output module. The specific overall structure of the system is shown in Figure 1.

The system hardware is mainly composed of three parts of circuits: image information acquisition circuit, image storage circuit, and tracking result output display circuit.

The tracking result output display circuit is mainly used to receive the digital image signals processed by the electronic derotation algorithm and the line and field synchronization signals of the data clock and convert these signals into analog image signals. The specific hardware structure is shown in Figure 2.

For the image recognition module, it is to detect the characteristic edges of the image accordingly to conduct

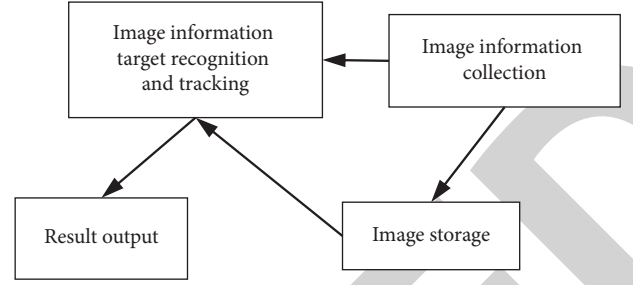


FIGURE 1: The overall structure of the system.

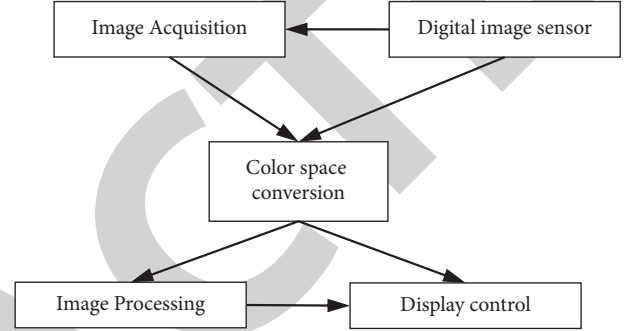


FIGURE 2: System hardware structure.

edge detection algorithms for different target objects. This method has higher efficiency and strong antiinterference, can smooth the noise, and can get edge information, so as to achieve the most efficient tracking; the specific structure is shown in Figure 3:

4.1. Image Recognition Module Design. The so-called image recognition is based on the detection of the edge of the image, and the detected edge is between the image and the image background, so it is a collection of pixel points according to the gray value of pixel. For the collected images, first of all, the corresponding operators need to be used to calculate the horizontal and vertical convolution of the two gradients, the second step is to merge the results of the gradient convolution, and finally, the edge pixels of the background image are obtained according to the corresponding threshold setting; finally, the result of the edge detection is obtained. The specific edge detection block diagram is shown in Figure 4:

For the pixel point calculation, a linear buffer is used for calculation, which is specifically 9 pixels, as shown in Figure 5:

The horizontal gradient operator is shown in Figure 6.

According to the edge detection algorithm, the G_x component of I5 can be calculated using the following formula:

$$\begin{aligned} G_x &= V_{I1} \times V_{T1} + V_{I2} \times V_{T2} + V_{I3} \times V_{T3} \\ &+ V_{I4} \times V_{T4} + V_{I5} \times V_{T5} \\ &+ V_{I6} \times V_{T6} + V_{I7} \times V_{T7} + V_{I8} \times V_{T8} + V_{I9} \times V_{T9}. \end{aligned} \quad (17)$$

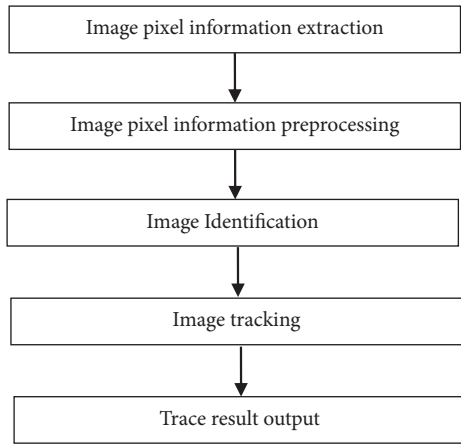


FIGURE 3: System software architecture.

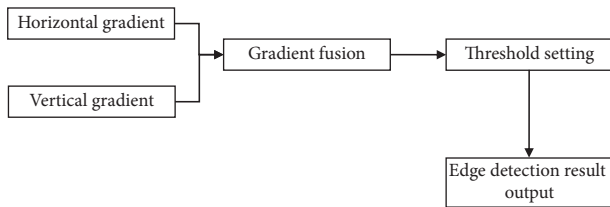


FIGURE 4: Block diagram of edge detection.

I1	I2	I3
I4	I5	I6
I7	I8	I9

FIGURE 5: List of image areas.

T1	T2	T3
T4	T5	T6
T7	T8	T9

FIGURE 6: Horizontal gradient operator.

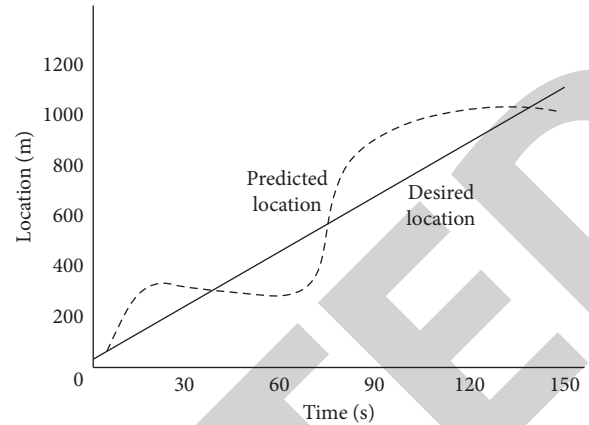


FIGURE 7: Position curve of the electronic derotation algorithm.

4.2. *Image Track.* Image tracking generally has two methods, based on the model matching and tracking method based on motion parameter estimation. This system studies tracking methods based on model matching. This tracking method can be divided into two types. One is the tracking algorithm based on the edge feature information of the target image. This algorithm is widely used, but it is susceptible to interference and can easily cause target tracking. The other is a tracking algorithm based on the feature information of the target image area. This algorithm has strong antiinterference ability and is very stable in tracking the target image in a complex background.

5. Simulation Experiment Analysis

The accuracy of automatic image recognition and tracking using the electronic derotation algorithm is higher than that of simple tracking using filtering. The main reason is that moving images can be obtained for image recognition, which can separate the background and foreground and then recognize motion tracking. The feature points of each moving image are matched separately, so that the accuracy of image recognition is higher.

The specific simulation experiment results are shown in Figures 7–10. The position obtained by the tracking algorithm is compared with the error curve.

By analyzing the results of Figures 7–10, under different simulation experiments, image recognition methods are used to visualize the position and trend curves. From the results, the trends of the two curves are basically the same. From the error position curve, it can be seen that it is compared with the actual position. The error is very small; this is through the threshold segmentation of the digital image, and the normalized calculation of the image is realized. The corresponding algorithm is used to identify the initial position of the moving image, and at the same time, the calculation function of the tracking target is obtained through the electronic derotation algorithm and the mean value theory to realize the tracking and positioning of the position.

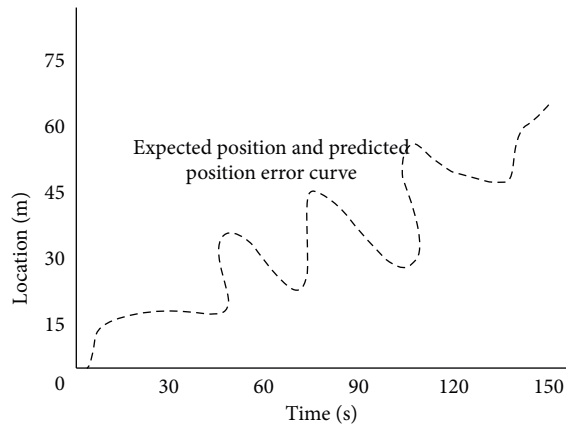


FIGURE 8: Position error curve of the electronic derotation algorithm.

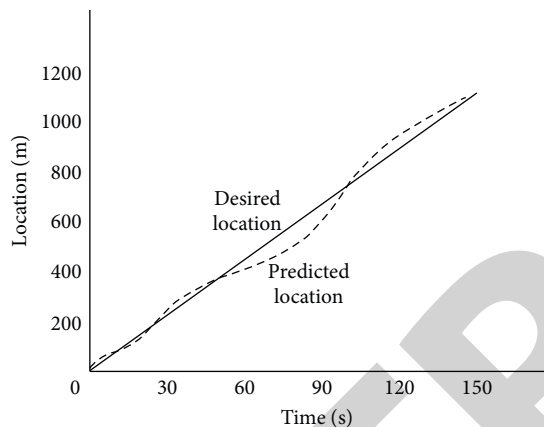


FIGURE 9: Position curve of the electronic derotation algorithm.

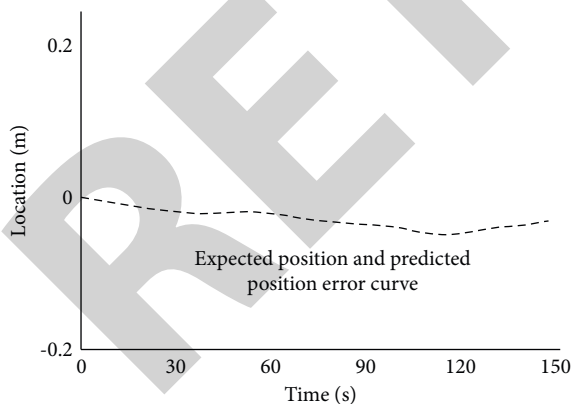


FIGURE 10: The position error curve of the electronic derotation algorithm.

6. Conclusions

Digital image recognition is an important step in mining and discovery of digital image information and is also a key difficulty in digital image research. Based on the electronic derotation algorithm, the image acquisition, color

conversion, and image processing are analyzed through sorting out the edge features of the digital image. The edge features of the image are analyzed, and effective and stable tracking is performed, which can accurately and effectively track the target object. Simulation experiments show that the electronic derotation algorithm is effective and can support the automatic recognition and tracking of digital images.

Data Availability

The data used to support the findings of this study are available from the corresponding author upon request.

Conflicts of Interest

The authors declare that they have no conflicts of interest.

Acknowledgments

The authors thank the financial support provided by Baoji University of Science and Arts Key Subject project (ZK2018010) and the project Application of PLC Technology in Automatic Control System (208010430).

References

- [1] C. Chattopadhyay and S. Das, "Supervised framework for automatic recognition and retrieval of interaction: a framework for classification and retrieving videos with similar human interactions," *IET Computer Vision*, vol. 10, no. 3, pp. 220–227, 2016.
- [2] Y. Tao and F. Zhou, "Autonomous space target recognition and tracking approach using star sensors based on a Kalman filter," *Applied Optics*, vol. 54, no. 11, pp. 3455–3462, 2015.
- [3] S. Wang, F. Jiang, and B. Zhang, "Development of UAV-based target tracking and recognition systems," *IEEE Transactions on Intelligent Transportation Systems*, vol. 2, no. 99, pp. 1–14, 2019.
- [4] X. Zhang, X. Kang, and N. Feng, "Automatic recognition of dairy cow mastitis from thermal images by a deep learning detector," *Computers and Electronics in Agriculture*, vol. 178, no. 2, pp. 315–326, 2020.
- [5] A. Yang, H. Huang, B. Zheng et al., "An automatic recognition framework for sow daily behaviours based on motion and image analyses," *Biosystems Engineering*, vol. 192, no. 4, pp. 56–71, 2020.
- [6] H. Kim, J. Han, and Y. J. Han, "Machine vision-driven automatic recognition of particle size and morphology in SEM images," *Nanoscale*, vol. 12, no. 2, pp. 1–12, 2020.
- [7] X. Jia, X. Mai, Y. Cui et al., "Automatic polyp recognition in colonoscopy images using deep learning and two-stage pyramidal feature prediction," *IEEE Transactions on Automation Science and Engineering*, vol. 2, no. 99, pp. 1–15, 2020.
- [8] Y. Wang, L. Mao, M.-A. Yu, Y. Wei, C. Hao, and D. Dong, "Automatic recognition of parathyroid nodules in ultrasound images based on fused prior pathological knowledge features," *IEEE Access*, vol. 9, no. 4, pp. 69626–69634, 2021.
- [9] Z. Chen, G. Huang, and C. Lu, "Automatic recognition of weld defects in ToFD D-scan images based on faster R-CNNs," *Journal of Testing and Evaluation*, vol. 48, no. 2, pp. 3210–3218, 2020.
- [10] "Automatic segmentation and Analysis of renal calculi in medical ultrasound images," *Pattern Recognition and Image Analysis*, vol. 30, no. 4, pp. 748–756, 2020.

- [11] J. Zhang, R. Jiang, and B. Li, "An automatic recognition method of microseismic signals based on EEMD-SVD and ELM," *Computers & Geosciences*, vol. 133, no. 12, pp. 1–11, 2019.
- [12] Y. Guo, X. Ge, and M. Yu, "Automatic recognition method for the repeat size of a weave pattern on a woven fabric image," *Textile Research Journal*, vol. 89, no. 4, pp. 95–103, 2018.
- [13] L. C. Ngugi, M. Abelwahab, and M. Abo-Zahhad, "Recent advances in image processing techniques for automated leaf pest and disease recognition - a review," *Information Processing in Agriculture*, vol. 86, no. 3, pp. 75–84, 2020.
- [14] G. Silvano, V. Ribeiro, V. Greati et al., "Synthetic image generation for training deep learning-based automated license plate recognition systems on the Brazilian Mercosur standard," *Design Automation for Embedded Systems*, vol. 25, no. 2, pp. 113–133, 2021.
- [15] Y. . Shi, "Image recognition of competitive aerobics movements based on embedded system and digital image processing," *Microprocessors and Microsystems*, vol. 82, no. 2, pp. 44–56, 2021.
- [16] A. B. Rosenkrantz, E. Johnson, and J. J. Sanger, "Use of a web-based image reporting and tracking system for assessing abdominal imaging examination quality issues in a single practice," *Abdominal Imaging*, vol. 40, no. 8, pp. 3354–3358, 2015.
- [17] B. N. Mohammed and H. B. Ahmad, "Advanced car-parking security platform using Arduino along with automatic license and number recognition," *Academic Journal of Nawroz University*, vol. 10, no. 1, pp. 1–12, 2021.
- [18] C. Xu, L. N. Govindarajan, and Y. Zhang, "Depth image based articulated object pose estimation, tracking, and action recognition on lie groups," *International Journal of Computer Vision*, vol. 123, no. 3, pp. 1–25, 2016.
- [19] K. Picos, U. Orozco-Rosas, V. H. Díaz-Ramírez, and O. Montiel, "Pose estimation in noncontinuous video sequences using evolutionary correlation filtering," *Mathematical Problems in Engineering*, vol. 2018, no. 7, pp. 1–13, 2018.